PHYSICAL REVIEW B VOLUME 56, NUMBER 4 15 JULY 1997-II

Transport properties of lightly doped $CoSb_3$ single crystals

E. Arushanov,* K. Fess, W. Kaefer, Ch. Kloc, and E. Bucher
Faculty of Physics, University of Konstanz, P.O. Box 5560, D-78434 Konstanz, Germany

(Received 27 December 1996; revised manuscript received 24 February 1997)

$CoSb_3$ single crystals with low hole concentration (down to 10^{17} cm^{-3}) at 300 K and 2.6×10^{16} cm^{-3} at 90 K) and the highest observed value of the room-temperature hole mobility (the value is up to 6000 $cm^2/V\,s$, i.e., up to about 1.8 times higher than maximum values previously reported) were grown. The observed temperature dependence of the Hall coefficient is explained assuming the existence of an acceptor impurity band and an additional deep acceptor level. The values of the activation energies of the shallow and deep acceptors, their concentrations, as well as the concentration of the compensating donors were calculated. It is shown that the scattering due to polar optical phonons and nonpolar optical phonons is most important in the high-temperature region. The value of the valence-band deformation potential is estimated. [S0163-1829(97)04427-5]

I. INTRODUCTION

$CoSb_3$ has attracted attention recently as potentially new thermoelectric material[1–5] and due to its unusual band-structure features.[6] The proximity of the linear-dispersion region near the band edge makes the skutterudite antimonides unique.[6] Single crystals of $CoSb_3$ were grown by the chemical vapor transport technique using chlorine as the transport agent[7] and from Sb-rich melt.[1–4,8] The room-temperature Hall mobility value is up to about 3000 $cm^2/V\,s$ in the $10^{17}-10^{18}$ cm^{-3} carrier-concentration range and decreases with increasing carrier concentration.[4] An exceptionally high value (3445 $cm^2/V\,s$ at 300 K at a carrier concentration of 4×10^{17} cm^{-3}) was reported by Caillat, Fleurial, and Borshevsky.[8] The lightly doped $CoSb_3$ single crystals [$p=(7-10)\times10^{16}$ cm^{-3} at 150–300 K (Ref. 3)] show that the Hall mobility peaks at 250 K at a value of 1940 $cm^2/V\,s$. The transport properties of p-type $CoSb_3$ single crystals were investigated.[1–5] Data on the scattering mechanisms are few and the results obtained are not in conformity with one another.

Morelli *et al.*[2] recently studied $CoSb_3$ samples with hole concentrations in the range of $2.6\times10^{17}-4.1\times10^{18}$ cm^{-3}. The temperature dependence of the hole mobility suggests a combination of scattering processes by phonons at high temperatures (above 100 K) and neutral impurities below 100 K. The absence of ionized impurity scattering in the samples studied is pointed out.

Caillat, Borshevsky, and Fleurial[4] have reported that the hole mobility in samples with hole concentration of $1.2\times10^{17}-9.4\times10^{18}$ cm^{-3} follows reasonably well a $T^{-3/2}$ behavior between 300 and 500 K which indicates that the predominant carrier scattering mechanism is acoustic-phonon scattering.

Mandrus *et al.*[3] have studied lightly doped $CoSb_3$ single crystals and came to the conclusion that the temperature dependence of the resistivity, Hall coefficient, Seebeck coefficient, and Hall mobility clearly reflects the dominance of ionized impurity scattering below 200 K. Above 200 K, the mobility begins to decrease with temperature, which most likely is due to the sudden influence of electrons on the Hall coefficient as the intrinsic regime is entered.

We present transport measurements on lightly doped p-type $CoSb_3$ single crystals. The observed room-temperature mobility is up to 6000 $cm^2/V\,s$, i.e., up to about 1.8 times higher than the already exceptionally high value previously reported.[8] Our data are discussed assuming the existence of an impurity band. To get more precise data on the scattering mechanisms in $CoSb_3$ single crystals, the analysis of mobility is performed taking into account acoustic, nonpolar, and polar optical phonon scattering as well as scattering by ionized impurities.

II. RESULTS AND DISCUSSION

$CoSb_3$ single crystals were grown by chemical vapor transport (CVT) reaction in closed silica ampoules and by flux in Sb-rich melts.[9] The samples were characterized by x-ray powder diffraction and energy dispersive x-ray analysis (EDX). In Fig. 1, the x-ray diffraction patterns for flux and CVT grown crystals are shown. The lattice constants were determined by a least-squares-fit method to 9.036 Å for both measurements. This is in good accordance with literature.[3,4] Both patterns give no indication of additional phases (e.g., excess Sb). The polished samples, which were used for the transport measurements were investigated under an optical microscope. There was again no precipitations. The EDX measurements revealed that the exact stoichiometry was given within the accuracy of the method. The resistivity ρ and the Hall coefficient R were measured in the temperature range from 4 to 400 K in a dc magnetic field H of 6000 Oe.

The $R(1/T)$ temperature dependence shows an exponential growth with decreasing temperature and a maximum at low temperatures (Fig. 2). The $1/T$ dependence of the resistivity is nearly exponential in the two temperature ranges (Fig. 3). The slope change of the $\rho(1/T)$ curves is observed near the temperatures corresponding to the maximum of the Hall coefficient.

The value of $\mu_H=R/\rho$ increases with increasing temperature, reaches a maximum (up to 8000 $cm^2/V\,s$) at about 200–400 K and decreases as T^{-n} (where $n=1.1$) in the lightest doped sample down to 6000 $cm^2/V\,s$ at room temperature (Fig. 4).

The observed features of $R(T)$ as well as the character of

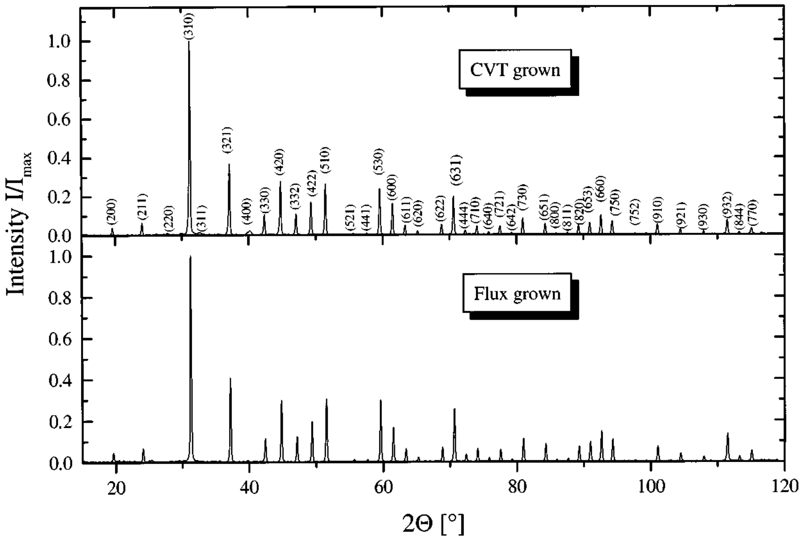

FIG. 1. X-ray diffraction powder patterns of CVT (batch 6) and flux grown (batch 4) $CoSb_3$. All peaks could be indexed in the skutterudite phase.

the temperature dependence of $\rho(T)$ and $R/\rho(T)$ could be explained assuming the existence of an impurity band formed by shallow impurity levels.[10–14] However, it is worth mentioning that the value of the activation energy, estimated on the basis of the high-temperature (higher than $R_{\max}$) Hall coefficient data is more than an order of magnitude higher than the value derived from the low-temperature (lower than $R_{\max}$) region. This suggests the existence of an additional deep acceptor level.

The carrier density as a function of temperature is given by the following expression for the approximation of the two acceptor and one donor levels:[15]

$$p+N_d=\frac{N_{A_1}}{1+\dfrac{\gamma p}{N_v}\exp\left(\dfrac{\varepsilon_1}{kT}\right)}+\frac{N_{A_2}}{1+\dfrac{\gamma p}{N_v}\exp\left(\dfrac{\varepsilon_2}{kT}\right)}, \tag{1}$$

where $N_v=2(2\pi m^* kT/h)^{3/2}$.

$N_{A_{1,2}}$ is the concentration of the shallow and deep acceptor levels, respectively; $\varepsilon_{1,2}$ is the activation energy of the shallow and deep acceptor levels, respectively; N_v is the density of states in the valence band, γ is the degeneracy factor ($\gamma=2$), and N_d is the concentration of compensating donors.

At high temperatures, where the impurities are depleted,

$$p=\frac{1}{eR_d}=N_{A_1}+N_{A_2}-N_d, \tag{2}$$

where R_d is determined from an extrapolation of $R(1/T)$ to $(1/T)\rightarrow 0$. At low temperatures, where it is possible to neglect the second term of the right-hand-side of Eq. (1), this expression reduces to

$$p+N_d=\frac{N_{A_1}}{1+\dfrac{\gamma p}{N_v}\exp\left(\dfrac{\varepsilon_1}{kT}\right)}, \tag{3}$$

and in the carrier freezing region

$$p_f=\frac{1}{eR_f}=N_{A_1}-N_d, \tag{4}$$

where R_f is the smallest value of R at low temperatures.

At high temperatures, assuming that

$$p \gg N_d, \quad \frac{\gamma p}{N_v}\exp\left(\frac{\varepsilon_2}{kT}\right) \gg 1,$$

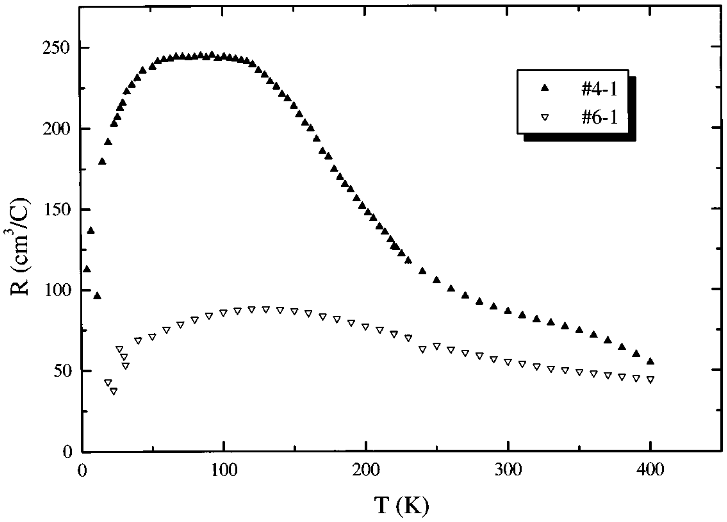

FIG. 2. Temperature dependence of the Hall coefficient. Here and hereafter the number of the curves correspond to the sample number.

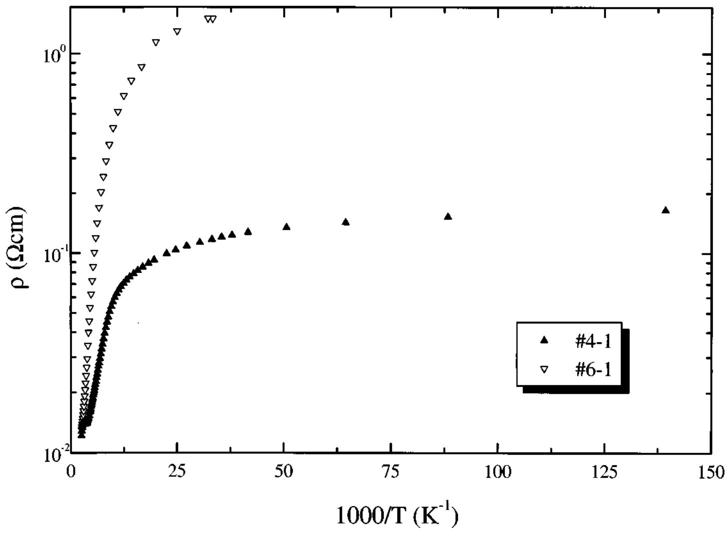

FIG. 3. Temperature dependence of the resistivity.

Eq. (1) can be written as

$$p=\left[\frac{N_v}{\gamma}N_{A_2}\right]^{1/2}\exp\left[-\frac{\varepsilon_2}{2kT}\right]. \tag{5}$$

In our samples the dependence of $p/T^{3/4}$ on $1/T$ is a straight line at high temperatures in accordance with Eq. (5), which confirms the assumptions made and permits us to determine the values of ε_2. The value of N_{A_2} was estimated using Eqs. (2) and (4).

An analysis of $R(T)$ at low temperatures has been made on the basis of a two-band model. In accordance with the method presented in Ref. 14, the temperature dependence of p, the hole concentration in the main (valence) band, and p_1, the hole concentration in the impurity band, were calculated (Fig. 5).

We also performed magnetic-field-dependent measurements of the Hall coefficient from 0 to 0.75 T at different temperatures. The results of these measurements are depicted in Fig. 6. No field dependence could be observed at high temperatures. At low temperatures, where the influence of the two-band conduction should be largest, a small increase of the Hall coefficient with the magnetic field was found. This increase could be due to the conduction in the two different bands, as proposed in the presented model.

At low temperatures, the temperature dependence of p is determined by Eq. (3), which can be written as

$$p=\frac{N_v}{\gamma}\,\frac{N_{A_1}-N_d}{N_d}\exp\left[-\frac{\varepsilon_1}{kT}\right], \tag{6}$$

assuming that $p \ll N_d$.

Using Eq. (6), the values of ε_1 as well as $N_v(N_{A_1}-N_d)/N_d$ were estimated. The latter permits the reader to calculate the value of N_d taking into account Eq. (4), if the value of m^*/m_0 is known.

The value of m^*/m_0 was estimated using the thermoelectric power α (Fig. 7) and Hall coefficient measurements. The reduced Fermi level η^* has been determined from Eq. (7) (Ref. 16)

$$\alpha=\frac{k}{e}\left(\frac{F_{r+2}}{F_{r+1}}-\eta^*\right), \tag{7}$$

where F_{r+m} are the Fermi-Dirac integrals, and r is the scattering factor. The values of r are equal to 0, 1, or 2 for

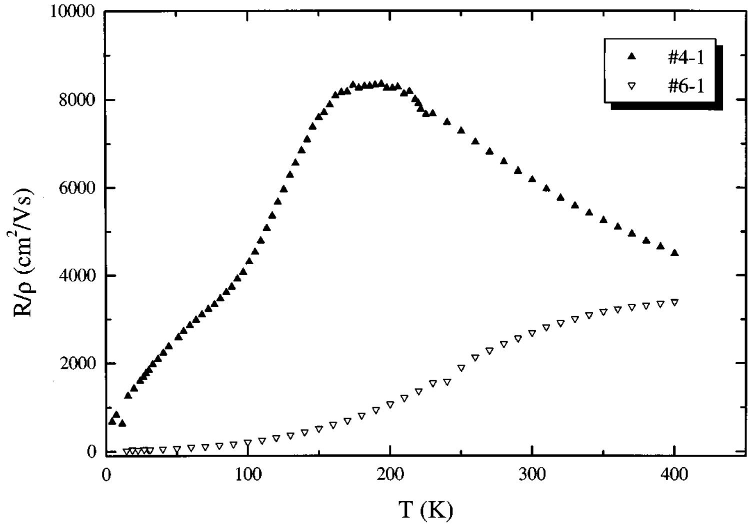

FIG. 4. Temperature dependence of R/ρ.

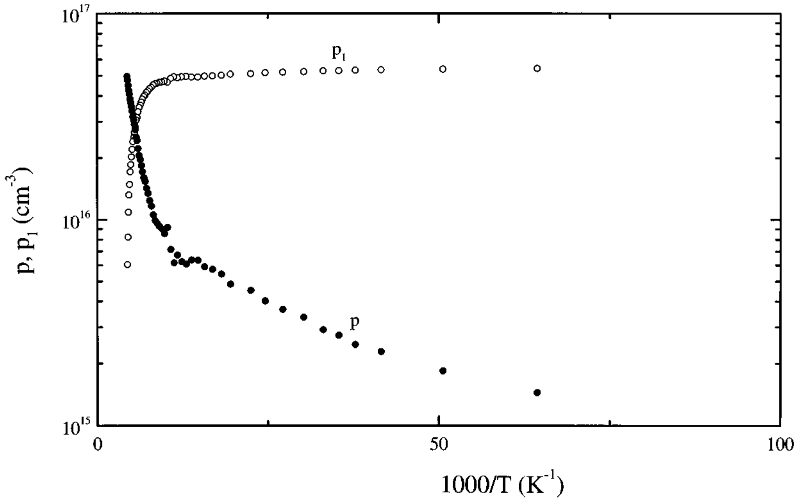

FIG. 5. Hole concentration p and p_1 vs temperature for Sample 4-1.

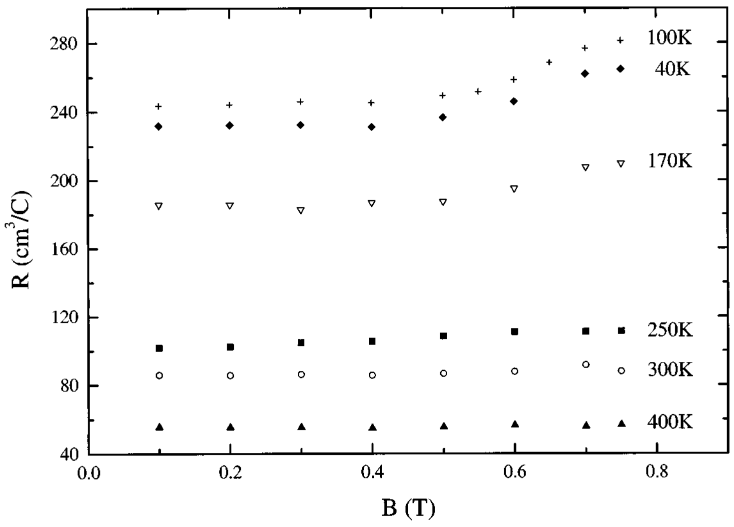

FIG. 6. Magnetic-field dependence of the Hall coefficient at different temperatures for sample 4-1.

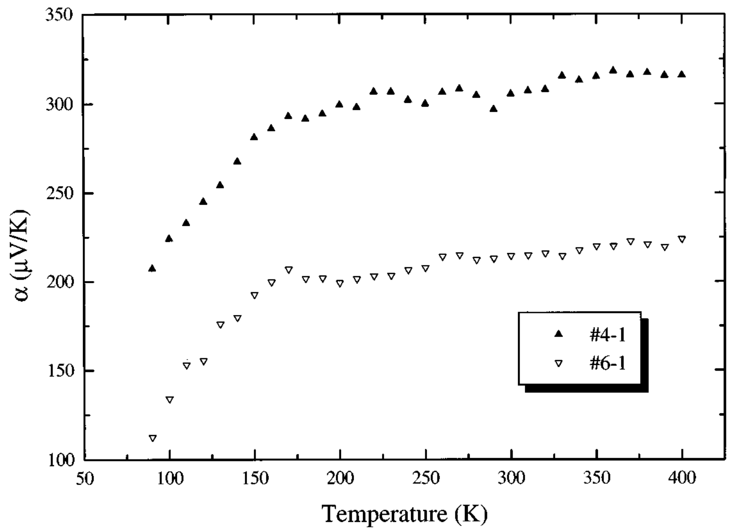

FIG. 7. Temperature dependence of the thermoelectric power.

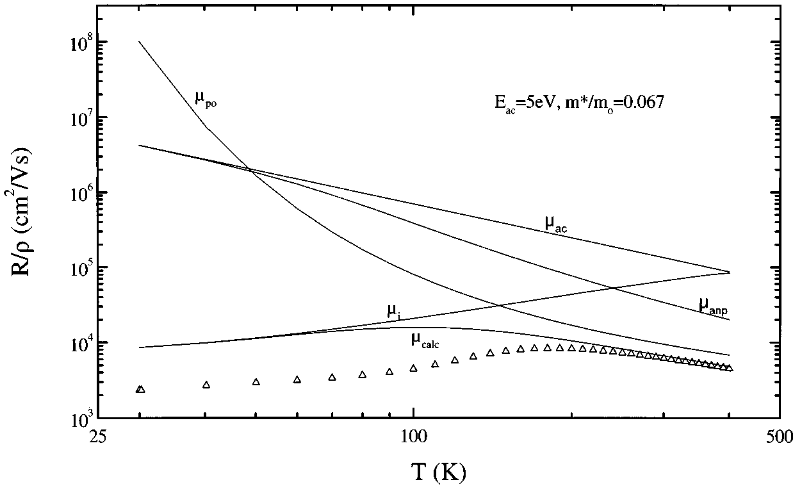

FIG. 8. Temperature dependence of R/ρ for sample 4-1.

scattering by acoustical, optical lattice vibrations at temperatures higher than the Debye temperature, and by ionized impurities, respectively.[16]

The upper limit of m^* calculated from Eqs. (7) and (8),

$$p=\frac{(2m^*kT)^{3/2}}{3\pi^2\hbar^3}F_{3/2}(\eta), \tag{8}$$

assuming $r=0$, is used to estimate the upper limit of N_d and N_{A_1}.

It is worth mentioning that the lightly doped CoSb$_3$ single crystal, studied by Mandrus *et al.*,[3] shows the same character of the temperature dependence of the Hall coefficient as our samples. That is why the same model has been applied to estimate its parameters (sample $m1$, Table I). The obtained set of parameters (N_{A_1}, N_{A_2}, N_d, $k=N_d/N_{A_1}$, ε_1, ε_2) is in reasonable agreement (Table I).

The value of ε_2 is about 50±10 meV. The same value was estimated from the temperature-dependent resistivity of the lightly doped CoSb$_3$ single crystals in the low-temperature region.[3] In Ref. 3 it is mentioned that the obtained value of the activation energy is in agreement with a recent band-structure calculation of CoSb$_3$ performed by Singh and Pickett[6] in which they predict a 50-meV semiconducting gap sided by two large peaks in the density of states separated by 0.50 eV. However, the data available are not conclusive enough to draw a final conclusion about the nature of the 50 meV activation energy.

The availability of high-quality CoSb$_3$ single crystals permits the reader to obtain more reliable data on the scattering mechanisms in the material studied. In order to estimate the strength of the different scattering mechanisms, the total mobility is calculated using Matthiessen's approximation:

$$\mu^{-1}=\mu_{\rm ac}^{-1}+\mu_{\rm npo}^{-1}+\mu_{\rm po}^{-1}+\mu_i^{-1}, \tag{9}$$

where $\mu_{\rm ac}$, $\mu_{\rm npo}$, $\mu_{\rm po}$, and μ_i are the mobilities of the charge carriers due to scattering by acoustic lattice modes, nonpolar optical modes, polar optical modes, and ionized impurities, respectively.

For the acoustic mode scattering mobility, the expression[17] is used

$$\mu_{\rm ac}=\frac{(8\pi)^{1/2}e\hbar^4\rho_0u^2}{3(kT)^{3/2}E_{\rm ac}^2(m^*)^{5/2}}, \tag{10}$$

where ρ_0 is the density, u is the longitudinal velocity of sound, and $E_{\rm ac}$ is the valence-band deformation potential.

The combined effect of the acoustic and nonpolar optical modes scattering contribution to the total mobility is given by[18]

$$\mu_{\rm acnpo}=\mu_{\rm ac}S(\theta,\eta,T), \tag{11}$$

where θ is the Debye temperature and $\eta=(E_{\rm npo}/E_{\rm ac})^2$ the squared ratio of the nonpolar optical and acoustic mode deformation potentials. $S(\theta,\eta,T)$ can be approximated to

$$S(\theta,\eta,T)\approx(1+A\eta)^{-1}, \tag{12}$$

with $A=Hz/(e^z-D)$, where H and D are tabulated for each value of η and $z=\theta/T$.

The mobility due to scattering of holes by polar optical phonons is[19]

$$\mu_{\rm po}=\frac{8\hbar^2T^{1/2}}{3(2\pi k)^{1/2}e\theta(m^*)^{3/2}}\left(\frac{1}{\varepsilon_\infty}-\frac{1}{\varepsilon_0}\right)^{-1}(e^z-1)G(z), \tag{13}$$

TABLE I. Parameters of p-type CoSb$_3$ single crystals.

Sample	N_{A_1} (10^{17} cm^{-3})	N_{A_2} (10^{17} cm^{-3})	N_d (10^{17} cm^{-3})	N_d/N_{A_1} (%)	ε_1 (meV)	ε_2 (meV)
4-1	1.5	1.37	0.93	62	<1	47
6-1	3.1	1.24	1.62	52	<1	38
$m1$	1.92	6.6	0.68	34	4	64

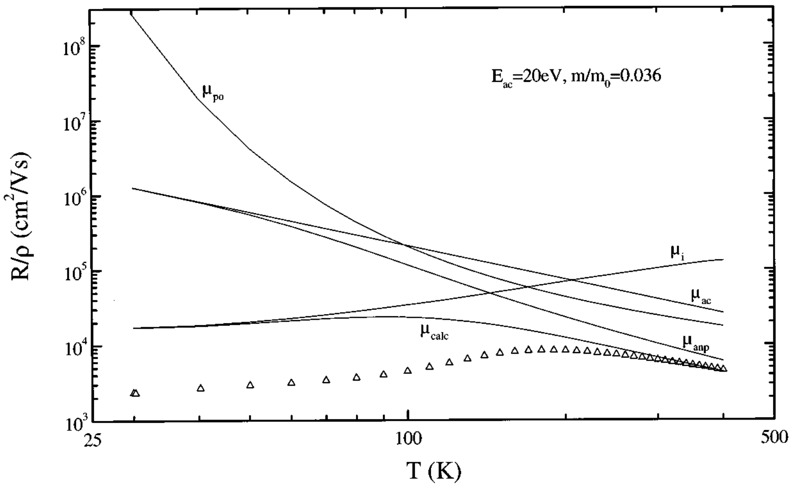

FIG. 9. Temperature dependence of R/ρ for sample 4-1.

where ε_∞ is the high-frequency dielectric constant and $G(z)$ is a tabulated function which may be approximated in the range of 100–300 K by $0.56+(26.93/T)$.

The Hall mobility due to ionized impurity scattering was calculated according to the Brooks-Herring formula:[20]

$$\mu_i=\frac{2^{7/2}\varepsilon_0^2(kT)^{3/2}}{\pi^{3/2}e^3(m^*)^{1/2}N_i f(x)}, \tag{14}$$

where $N_i=2N_d+p$ is the concentration of the ionized impurities. The function $f(x)$ is given by the relation $\ln(1+x)-x/(1+x)$ where,

$$x=6\varepsilon_0 m^*(kT)^2/\pi e^2h^2p.$$

To make a fit to the mobility data, the following set of parameters has been used; $\rho_0=7.64$ g/cm^3,[7] $\theta=306$ K,[2] $\varepsilon_0=33.5$,[21] $\varepsilon_\infty=25$,[21] H, D, and η are equal to 1.34, 0.914, and 4, respectively.[18] The value of ε_0 was calculated, using data on lattice vibrations in CoSb$_3$ and the Lyddane-Sachs-Teller relation:[22]

$$\frac{\varepsilon_0}{\varepsilon_\infty}=\prod_i\left(\frac{\omega_{\mathrm{LO}}}{\omega_{\mathrm{TO}}}\right)_i^2,$$

where ω_{LO} and ω_{TO} are LO and TO phonon frequencies.

The sound velocity is estimated as[23]

$$u\cong\frac{k\theta}{h}\left(\frac{V}{6\pi^2}\right)^{1/3},$$

where V is the average atomic volume.

The value of m^*/m_0 was estimated using Eqs. (7) and (8). Taking into account that the mobility in the high-temperature region increases with decreasing temperature as T^{-n} ($n=1.1$, sample 4-1), the scattering factor was assumed to be equal to 0 or 1. The value of m^*/m_0 is equal to 0.067 at $r=0$ and 0.036 at $r=1$ (sample 4-1). The values of E_{ac} and N_d were used as adjustable parameters to fit mobility data.

It is also worth mentioning that our samples (Figs. 2–4 and 7) do not show an intrinsic region in the studied temperature interval as it is indicated for the sample studied in Ref. 3.

The analysis of mobility data was performed assuming that the mobility is limited not only by acoustic lattice mode, but also by nonpolar optical and by polar optical modes. The values of E_{ac} ($E_{\mathrm{ac}}=5$ eV if $m^*/m_0=0.067$, Fig. 8, and $E_{\mathrm{ac}}=20$ eV if $m^*/m_0=0.036$, Fig. 9) and N_d ($N_d=7.9\times10^{16}$ cm^{-3}) were estimated from the fitting procedure. The obtained value of N_d is in satisfactory agreement with the value determined from the Hall coefficient data (Table I).

The scattering due to polar optical phonons and nonpolar optical phonons is most important at temperatures of 150–400 K (Figs. 8 and 9). The availability of a more exact value of m^*/m_0 is necessary to separate the contribution of these two scattering mechanisms. The calculated scattering contribution due to ionized impurities was found to be negligible at this temperature region. It is different from the results previously obtained which leads to the conclusion that the dominant scattering mechanisms are by acoustic phonon[2,4] or by ionized impurities.[3] The analysis of the scattering mechanisms in the low-temperature region is complicated due to the influence of the impurity band conduction.

III. SUMMARY

In summary, CoSb$_3$ single crystals with low hole concentrations (down to 10^{17} cm^{-3} at 300 K and 2.6×10^{16} cm^{-3} at 90 K) and high mobilities (the room-temperature hole mobility value is up to 6000 cm^2/V s, i.e., up to about 1.8 times higher than the exceptionally high value previously reported[8]) were grown. The observed temperature dependence of the Hall coefficient is explained within the limit of a two-acceptor–one-donor model. The value of the activation energy of the shallow and deep acceptors, their concentration, as well as the concentration of the compensating donors were calculated. The dominant scattering mechanisms were determined, using analysis of the Hall mobility data. The value of the valence-band deformation potential is estimated.

*Permanent address: Institute of Applied Physics, Academy of Sciences of Moldova, Kishinev, Moldova.

[1] T. Caillat, A. Borshevsky, and J.-P. Fleurial, in *Proceedings of the Eleventh International Conference on Thermoelectrics, Arlington, Texas, 1993*, edited by K. R. Rao (University of Texas Press, Arlington, 1993), p. 98.

[2] D. T. Morelli, T. Caillat, J.-P. Fleurial, A. Borshevsky, J. Vandersande, B. Chen, and S. Uher, Phys. Rev. B **51**, 9622 (1995).

[3] D. Mandrus, A. Migliori, T. W. Darling, M. F. Hundley, E. J. Peterson, and J. D. Thompson, Phys. Rev. B **52**, 4926 (1995).

[4] T. Caillat, A. Borshevsky, and J.-P. Fleurial, J. Appl. Phys. **80**, 4442 (1996).

[5] J. W. Sharp, E. C. Jones, R. K. Williams, P. M. Martin, and B. C. Sales, J. Appl. Phys. **78**, 1013 (1995).

[6] David J. Singh and Warren E. Pickett, Phys. Rev. B **50**, 11 235 (1994).

[7] J. Ackerman and A. Wold, J. Phys. Chem. Solids **38**, 1013 (1977).

[8] T. Caillat, J.-P. Fleurial, and A. Borshevsky, J. Cryst. Growth **166**, 722 (1996).

[9] Ch. Kloc, K. Fess, W. Kaefer, K. Friemelt, H. Riazi-Nejad, M. Wendl, and E. Bucher, in Proceedings of the Fifteenth International Conference on Thermoelectrics, Pasadena, California, 1996, edited by T. Laillat (IEEE, Piscataway, 1996), p. 155.

[10] C. S. Hung and J. R. Gliessman, Phys. Rev. **79**, 726 (1950).

[11] E. M. Conwell, Phys. Rev. **98**, 1178 (1955).

[12] O. V. Emelyanenko, T. S. Lagunova, D. N. Nasledov, and G. N. Talalakin, Fiz. Tverd. Tela **7**, 1315 (1965) [Sov. Phys. Solid State **7**, 1063 (1965)].

[13] I. K. Andronik, E. K. Arushanov, O. V. Emelyanenko, and D. N. Nasledov, Fiz. Tekh. Poluprovodn. **2**, 1248 (1968) [Sov. Phys. Semicond. **2**, 10 491 (1969)].

[14] E. Arushanov, Ch. Kloc, and E. Bucher, Phys. Rev. B **50**, 2653 (1994).

[15] J. S. Blakemore, *Semiconductor Statistics* (Pergamon Press, Oxford, 1962).

[16] B. M. Askerov, *Transport Phenomena in Semiconductors* (Nauka, Leningrad, 1970).

[17] J. Bardeen and W. Shockley, Phys. Rev. **77**, 407 (1950).

[18] J. D. Wiley and M. Di Domenico, Jr., Phys. Rev. B **2**, 427 (1970).

[19] H. Ehrenreich, J. Phys. Chem. Solids **2**, 131 (1957).

[20] H. Brooks, Adv. Electron. Electron Phys. **7**, 85 (1955).

[21] G. Kliche and H. D. Lutz, Infrared Phys. **24**, 171 (1984).

[22] W. Cochran and R. A. Cowley, J. Phys. Chem. Solids **23**, 447 (1962).

[23] J. R. Drabble and H. J. Goldsmid, *Thermal Conduction in Semiconductors* (Pergamon Press, Oxford, 1961), p. 191.